MASS-BALANCE ASPECTS OF WEDDELL SEA PACK ICE

By S. F. ACKLEY

(U.S. Army Cold Regions Research and Engineering Laboratory, Hanover, New Hampshire 03755, U.S.A.)

ABSTRACT. The Weddell Sea pack ice undergoes several unique advance–retreat characteristics related to the clockwise transport in the Weddell Gyre, the physical setting for the pack ice, and the free boundary with the oceans to the north. From satellite-derived ice charts, the annual cycle of the pack ice advance and retreat is depicted. The Weddell pack advance is characterized by a strong east-moving component as well as the north advance seen in other regions such as East Antarctica.

Physical characteristics of the pack ice at the summer minimum ice edge are presented. Indications are that deformation is a significant component of the ice accumulation, deformed ice accounting for *c.* 15 to 20% of the area covered in the year-round pack. Ablation characteristics are inferred from observations made during field work and from satellite imagery. These observations indicate that surface-melt ablation typically seen on Arctic pack is not seen on the Weddell pack inside the summer edge.

Using the physical-property data and transport inferred from ship and iceberg drifts, a new annual ice accumulation $\bar{\eta} > 3$ m is inferred over the continental shelf in the South compared to $\bar{\eta} < 2$ m previously estimated (Gill, 1973). The implication is that salt flux into the ocean over the shelf may be significantly larger, thereby increasing the production of Western Shelf Water, a component of Antarctic Bottom Water.

RÉSUMÉ. *Aspects du bilan de masse de la banquise de la Mer de Weddell.* La banquise de la Mer de Weddell est soumise à plusieurs systèmes d'influences pouvant provoquer avances ou retraits et liés au transport des glaces dans le sens des aiguilles d'une montre par le courant circulaire de Weddell, à la prise en masse physique de la glace du pack et à la libre communication avec les Océans du Nord. A partir de relevés par satellites on a retracé le cycle annuel de l'avancée et du recul de la glace de la banquise. L'avancée de la banquise de Weddell est caractérisée par une forte composante de son mouvement dirigée vers l'Est, ainsi que l'avancée vers le Nord observée dans d'autres régions telles que l'Antarctique de l'Est.

On présente les caractéristiques physiques de la banquise au moment du minimum estival de l'étendue de la glace. On a des indices selon lesquels la déformation est une composante significative de l'accumulation de la glace, la glace déformée comptant pour environ 15 à 20% dans la surface couverte par la banquise au long d'un cycle annuel. Les caractéristiques de l'ablation sont déduites d'observations faites sur le terrain et des images des satellites. Ces observations indiquent que l'ablation par fusion superficielle typique dans la banquise Arctique n'est pas sensible sur la banquise de Weddell à l'intérieur de ses limites estivales.

En utilisant des données sur les propriétés physiques de la glace et sur les transports décelés par l'observation de la dérive des navires et des icebergs, une accumulation annuelle de glace nouvelle $\bar{\eta} > 3$ m est supposée sur l'ensemble de la calotte continentale au Sud, au lieu d'une épaisseur précédemment estimée (Gill, 1973) à $\bar{\eta} < 2$ m. La conséquence est que le flux salé vers l'océan depuis la calotte peut être significativement plus important, et peut donc accroître le débit du courant du Western Shelf une composante du courant de fond Antarctique.

ZUSAMMENFASSUNG. *Gesichtspunkte zur Massenbilanz des Packeises in der Weddell-See.* Das Packeis der Weddell-See weist einige besondere Vorstoss- und Rückzugscharakteristiken auf, die mit dem Driften im Uhrzeigersinn innerhalb des Weddell-Kreisels, der physikalischen Verfassung des Packeises und den im Norden frei angrenzenden Meeren zusammenhängen. Der jährliche Zyklus des Packeisvorstosses und -rückgangs wird aus Eiskarten hergeleitet, die auf Satellitenbildern beruhen. Den Vorstoss bestimmt eine starke, nach Osten gerichtete Komponente, zusätzlich zur Bewegung nach Norden, die auch in anderen Gebieten, z.B. in der Ostantarktis festzustellen ist.

Für den Minimalstand des Eisrandes im Sommer werden die physikalischen Charakteristika angegeben. Der Anteil von 15 bis 20% deformierten Eises innerhalb des ganzjährig vom Packeis bedeckten Gebietes deutet darauf hin, dass die Deformation wesentlich zur Akkumulation des Eises beiträgt. Auf Ablations-charakteristiken wird aus Feldbeobachtungen und Satellitenbildern geschlossen. Diese Beobachtungen zeigen, dass Ablation durch Abschmelzen an der Oberfläche, wie sie für arktisches Packeis typisch ist, innerhalb des sommerlichen Eisrandes im Weddell-Packeis nicht auftritt.

Aus den physikalischen Eigenschaften und der Bewegung, die aus Schiffs- und Eisbergdriften zu erkennen ist, kann auf einen neuen Wert der jährlichen Eisakkumulation von mehr als 3 m über dem Kontinentalschelf im Süden geschlossen werden, gegenüber weniger als 2 m aus früheren Schätzungen (Gill, 1973). Eine Verwicklung besteht darin, dass der Salzausfluss über den Schelf in den Ozean wesentlich grösser sein und deshalb die Produktion von westlichen Schelfwasser, einen Teil des antarktischen Bodenwassers, erhöhen kann.
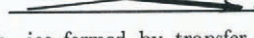
INTRODUCTION

The mass balance of a pack-ice region is important to understand since the balance in any particular region specifies a unique set of atmospheric and oceanic processes. Koerner's (1973) mass-balance study of the Arctic pack, for example, showed that ice deformation accounted for some 20% of the total annual ice production (accumulation). Annual variations in the ice

production were, therefore, more likely to be the result of changes in ridging and hummocking activity caused by wind and storm variability than of climatic variations in temperature, two distinctly different modes of atmospheric driving.

Schematically, the different modes of cooling or heating associated with ice transport take place as shown in Table I with the dark arrow indicating the dominant mechanism.

TABLE I. EFFECTS OF ICE FORMATION (SOURCE) AND DECAY (SINK) ON ATMOSPHERIC AND OCEANIC PROCESSES

Ice advection

SOURCE REGION – – – – – – – – – – SINK REGION

Atmospheric heating ⟶ Atmospheric cooling
Oceanic heating ⟶ Oceanic cooling

Atmospheric heating—ice formed by transfer of latent heat to the atmosphere (usual freezing mode)

Oceanic heating—frazil ice crystals are formed in the water column, by transferring latent heat to their water surroundings

Atmospheric cooling—ice cover melts from its top by extraction of heat from the atmosphere

Oceanic cooling—ice melts by mixing with ocean water, dissipating the radiational heat gain of the ocean in polar summer conditions

For the Northern Hemisphere, Hibler (1979), in a numerical simulation of the Arctic Basin ice, has shown this effect takes place through water freezing (atmospheric heating) in coastal regions of the Basin and melting (oceanic cooling) from ice transported out of the Basin through the Greenland–Svalbard passage. The other mechanisms depicted should not be neglected however, since, for example, the formation of melt ponds on the summer surface of the Arctic pack is an atmospheric cooling effect of considerable magnitude. Similarly, the formation of ice crystals in the water column (oceanic heating) is frequently observed in near-shore conditions in the Antarctic (Bunt, 1963).

In the Weddell Sea, one application of the mass balance is to understand the ice production over the continental shelf in the south. The ice accumulation in that area causes a salt flux into the water during freezing and creates a water type identified as Western Shelf Water, an essential component of Antarctic Bottom Water (Gill, 1973; Foster and Carmack, 1976). It is necessary to know both the production and the eventual disposition of the ice since it is probable that freezing and melting in the same region without ice transport would not change the water structure if the column is well mixed.

ANNUAL CYCLE CHARACTERISTICS OF THE WEDDELL SEA PACK ICE

The area defined as the Weddell Sea region (Ackley and Keliher, 1976), is bounded by the Antarctic Peninsula (long. 60° W.) on the west, and the Antarctic continent on the south. The northern boundary is the free boundary with the Atlantic and Indian Oceans without a topographic barrier to ice movement on the north. No topographic barrier exists on the eastern boundary which is set at long. 30° E. and is well out of the Weddell embayment (c. long. 20° W. to 60° W.) (Fig. 1). Work on the water circulation in the Antarctic regions defines the Kerguelen Plateau as the eastern boundary of the Weddell Gyre where southward flow, closing the Gyre's water circulation, is presumed to take place over a fairly broad region (Deacon, 1977; Gordon and others, 1978).

In Figure 1, we show "isochrones" of the ice edge in the Weddell Sea and East Antarctica during the advance period for 1974. The data are from ice extent charts compiled by U.S. Navy Fleet Weather Facility from several satellite data sources. The primary measurement
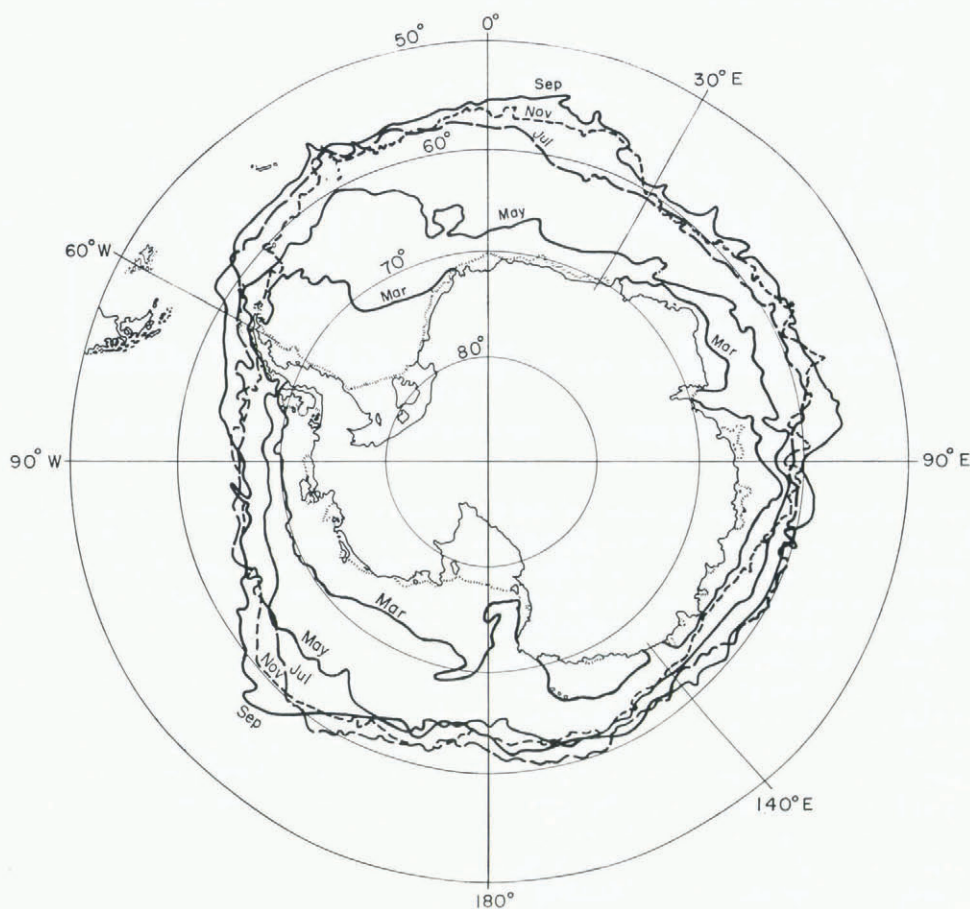
Fig. 1. Ice-edge isochrones during advance for 1974. The Weddell Sea region is bounded by the Antarctic Peninsula (long. 60° W.) and the 30° E. longitude line.

system in winter is a passive microwave radiometer aboard the Nimbus satellite (Zwally and Gloersen, 1977).

In Figure 2 the movement of the ice edge for particular longitudes (40° W., 20° W., 10° E., and 30° E.) is plotted against time and the characteristic east and north advance of the ice is seen. The advance phase is characterized by two east-moving components, the first appearing in the April–July period as the ice edge "front" passes successively from long. 40° W. → 20° W. → 10° E. As seen on Figure 2, the 30° E. advance in June–August nearly coincides with that of 10° E., is not as steep as the 40° W. → 20° W. → 10° E. advance, and is typical of the ice-edge movement from south to north off East Antarctica. A second wave or "front" is seen during the later winter–spring period (August–December). Here the maximum north point of the ice edge progressively moves from long. 20° W. (August) to 10° E. (October) finally passing 30° E. in December. The ice-edge movement at long. 30° E. strikingly illustrates the west-to-east character of the wave, since it passes long. 30° E. *after* the seasonal cycle has already started the southern retreat of the ice edge at this longitude in November. The result is two maxima in the long. 30° E. annual cycle, one in November
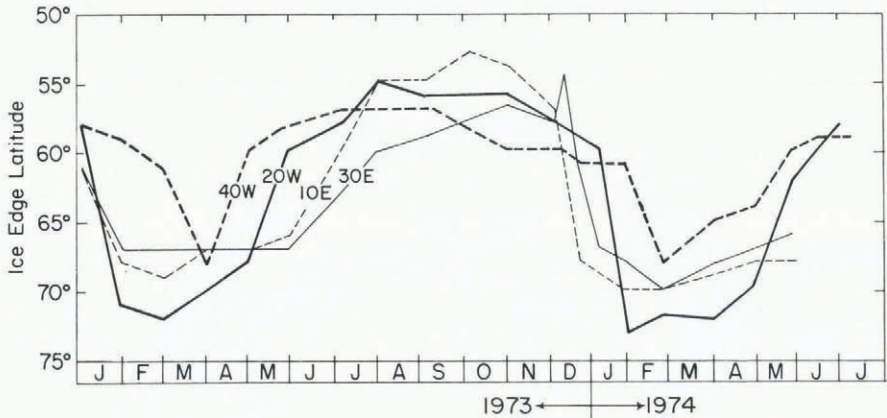
Fig. 2. Position of ice-edge latitude versus time for long. 40° W., 20° W., 10° E., and 30° E.

and one in December. The break-up of the ice is rapid at this time and the wave decays quickly, so "bumps" in the retreat–advance curves do not appear later than December at more easterly longitudes (e.g. none at long. 40° E.). The pulse of ice seen at long. 30° E. at the end of the spring season is support for including this longitude as the eastern boundary of the Weddell Sea region since it is the most easterly point to participate in the distinct advance characteristic of the Weddell Sea region as illustrated here.

From October through March, the pack is in its decay phase but, as indicated, the Weddell pack is characterized by a continuing advance of the edge position as an east-moving wave from October (long. 10° E.) to November (long. 20° E.) to December (long. 30° E.) with a simultaneous south-moving retreat of the ice edge in the western longitudes. Retreat continues south in the eastern longitudes and south-west in the western longitudes until the minimum extent is reached in March. In contrast, the advance isochrones for East Antarctica, also shown in Figure 1, are dominated by the northern advance without the north-east- and east-moving character seen for the Weddell Sea region.

Figure 3 indicates the area bounded by the pack ice as a function of time for the year 1974 also taken from the charts of ice extent. This figure shows the area change for East Antarctica (long. 30° E. to 140° E.) for comparison. As seen here, the total area of pack-ice coverage for the Weddell Sea region is approximately 7.5×10^6 km² at winter maximum and $< 2 \times 10^6$ km² at summer minimum. Compared to East Antarctica, the Weddell pack advances more rapidly during May through July and covers a greater area during winter. The difference (winter maximum area minus summer minimum area) is 6×10^6 km² for the Weddell Sea region while the same winter–summer difference is 4×10^6 km² for East Antarctica.
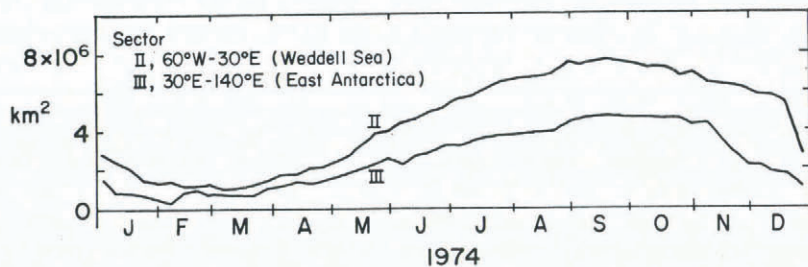

Fig. 3. Extent of pack ice versus time during 1974, for the Weddell Sea region and East Antarctica.

The distinctive features that give the Weddell Sea region its characteristically greater winter area coverage than East Antarctica are then: (1) the early-season advance at high latitudes which proceeds north-easterly and covers the Weddell Sea embayment (long. 20° W. to 60° W.) by mid-May; (2) penetration of the ice edge to the northern latitudes (lat. 58° S. to 55° S.) by a broad northern advance during mid-winter (July–September); (3) an east to north-east ice-edge advance into the eastern longitudes from lat. 55° S. into still lower latitudes (lat. 53° S.) during late winter and spring (September–December). These features contrast with the general advance of the ice edge directed from south to north at lower advance rates and with less area of ice coverage in the East Antarctic region.
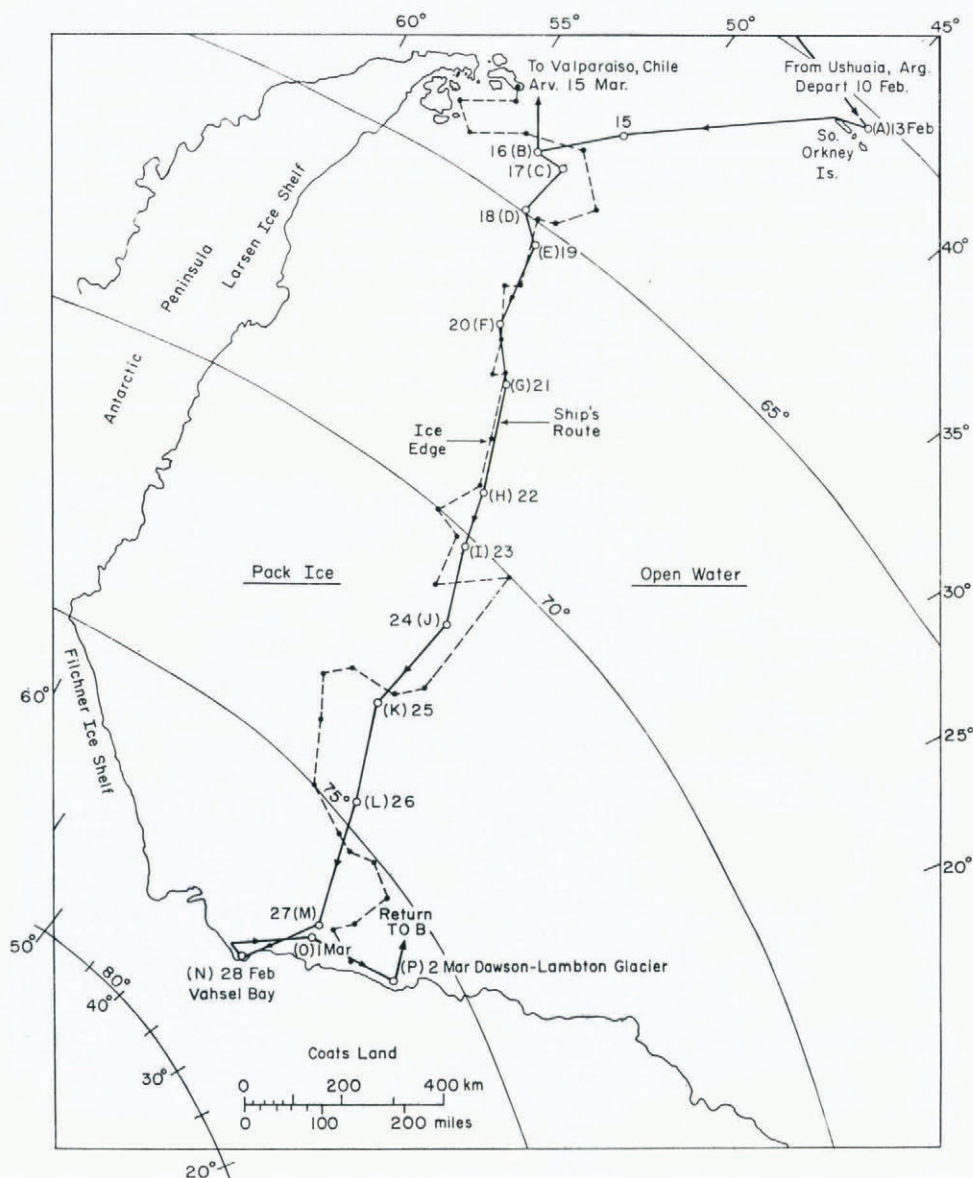

Fig. 4. Solid line shows the ship's track; dashed, the ice edge during U.S.C.G.C. Burton Island's *cruise during February/March* 1977.

PHYSICAL PROPERTIES OF WEDDELL PACK ICE

Figure 4 shows the cruise track taken during February 1977 by U.S.C.G.C. *Burton Island* in a field study (Ackley, 1977) to sample the properties of the pack ice. In this section, we report on these properties and the inferred mass-balance implications of the measured properties.

Accumulation characteristics

The primary accumulation characteristics of the region are given by the distribution of ice thickness and the amounts of ice involved in deformation. As shown in Figure 4, the sampling is taken only from the summer minimum regions of the ice edge. Figure 5 is from a photograph showing the ice typical of this region, taken a few tens of meters above the ice. The central floe is *c.* 25 to 30 m in its longest dimension. The ice consists of small floes up to *c.* 30 m across in a matrix of broken bits of ice and newly frozen thinner ice (gray–white, gray, and black ice). Measurements of thickness were taken from the thicker floes (e.g. the central floe in Fig. 5) and the thickness results are shown as a function of the sampled latitude in Figure 6. Efforts were made to sample the level ice away from ridges, blocks, depressions, and other obvious surface features. 51 floes were sampled and 139 holes are represented by the data in Figure 6. As indicated here, the ice thicknesses tend to be thickest in the north and thinner in the south, consistent, as we show in Figure 7, with a drift pattern for the region from south to north. By using the initial mean thickness of about 1.5–2.0 m in the southern region and assuming a floe residence of *c.* 1 year from the ship drift, the net mean accumulation is found to be between 0.5 to 1.5 m. This estimate is surprisingly large since significantly less accumulation is expected under thicker ice in its second winter (Thorndike and others, 1975).

Fig. 5. Photograph taken of the near-edge ice in the Weddell Sea from a helicopter. Large central floe is c. 25 to 30 m in its longest dimension.
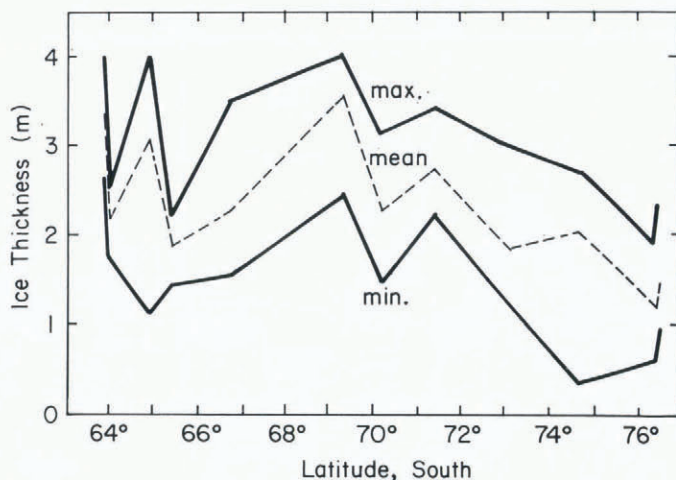
Fig. 6. *Ice thickness versus latitude from the track shown in Figure 4. Thicknesses were measured on the level portions of the older floes along the track such as the central floe in Figure 5.*

An important feature of the mass balance is the annual accumulation, but as we indicated earlier, the measured values given are only indicative of the older, level ice. Koerner (1973), Thorndike and others (1975), Maykut (1978), and Hibler (1979), have indicated the errors involved in inferring the characteristic behavior of the pack without appropriate consideration of the ice thickness distribution as well as the characteristics of old level ice.

Photographs such as that shown in Figure 5 were analyzed to give more complete information on the different types of ice and their percentages. The young ice appeared as gray–white areas in the photographs, and spot measurements taken in the field indicated thickness values continuously <1 m for this ice, usually falling in the range of 0.2 to 0.5 m. The older level ice (white) had thicknesses shown in Figure 6 with minimum values continuously above 1 m and usually above 1.5 m. The equipment was limited to sampling up to 4 m thicknesses, and thicknesses greater than this were encountered a few times without penetration through the ice, in locations such as near ridges. Although the data are indicative only of the ice-edge region and not of the interior regions, a thickness distribution for the ice edge may be useful for numerical simulation purposes and so is given here with that qualification. This distribution, shown in Figure 8, uses the format given by Maykut (1978) where the thickness intervals are doubled for each category. The errors on these categories can be quite significant but within the three broad categories shown are probably within $\pm 5\%$. The interior regions of the pack, in the absence of floe break-up by waves and swell and with less divergence than near the edge, probably have less percentage of young ice than those shown in Figure 8, more of older level ice, and about the same of ridged ice.

Ablation characteristics

Ablation was not directly measured, but is inferred from indirect measurements reported here.

The electronically scanning microwave radiometer (ESMR) on the Nimbus satellite gives some indication of the extent of ice melting by the behavior of the characteristic summer signal. According to Zwally and Gloersen (1977), a change in satellite-received signal characteristic of melt conditions on the continental ice adjacent to the Weddell pack occurs only at latitudes north of lat. 69° S., indicating that surface melt is confined to these more northern latitudes, at least on the continental ice.
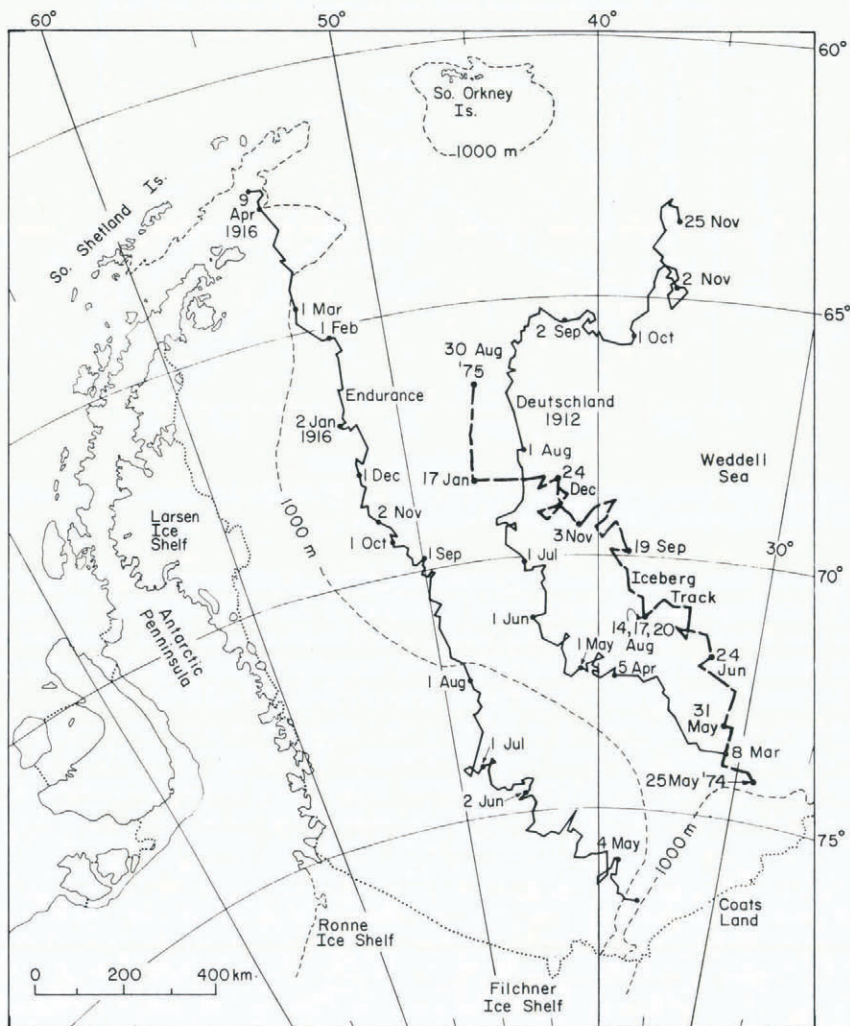
Fig. 7. Drift tracks of the ships Endurance *and* Deutschland *after they were trapped in the Weddell pack ice. An iceberg track obtained by satellite is also shown.*

Figure 9 shows two Landsat images over sea ice taken at respectively lat. 67° S. and 70° N. in the near-infrared band (MSS 7) of the system. Both images were obtained within 30 d after the summer solstice in their respective hemispheres, that is, at the time when surface melt conditions are expected to be in full swing. As shown here, the gray characteristics, indicating the melt ponds and generally wet surface conditions corresponding to surface melt ablation, are strongly evident for the Arctic image and absent from the Antarctic image, even though the Antarctic image is at a relatively lower latitude. The Landsat images indicating little surface melt are in agreement with the passive microwave observations that melting is low on the Weddell summer pack at the higher latitudes.

The field study indicated a relative lack of melt features with no observations of new or refrozen melt ponds or even wet surfaces over the length of the cruise track. These are biased toward the end of the summer period (mid-February) but, for the Arctic case, surface melt
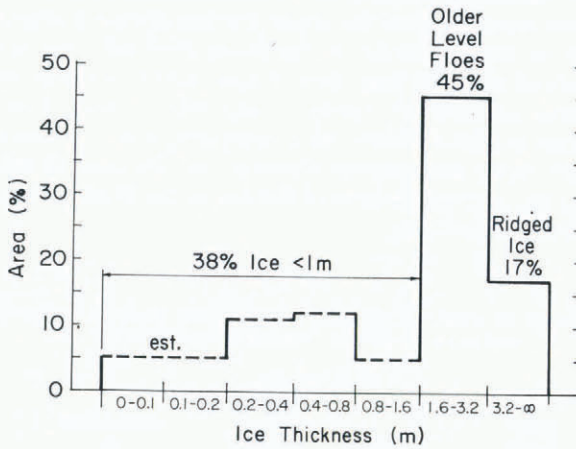
Fig. 8. *Estimated thickness distribution of the near-edge pack ice in the Weddell Sea.*

proceeds strongly for some sixty days past the summer solstice so, by analogy, some melt features might reasonably be observed in the Weddell Sea region during February. Additionally, as shown in Figure 5, new ice continues to form between the older floes indicating that sub-freezing temperatures are continuously present during the summer period considerably reducing the possible ablation. Foster (1972) reports direct observation of ice freeze-up events in the Weddell Sea in lat. 75–77° S. near the ice-shelf front in midsummer. Our observations are further north and imply that freezing is nearly continuous during summer in the pack-ice regions away from the ice shelf. Salinity distributions within the ice are also an indicator of ablation characteristics, since the onset of brine drainage precedes surface melt
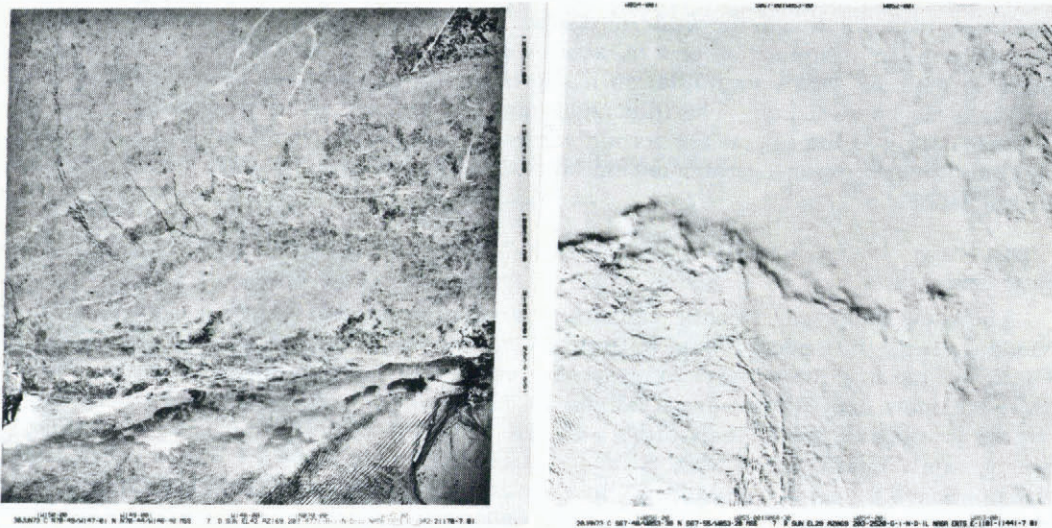

Fig. 9.
(a) *Landsat image from sea ice off the Alaskan coast at lat. 70° N., at summer solstice + 10 d, most sensitive to the presence of surface moisture.*
(b) *Landsat image from sea ice in the Weddell Sea taken at summer solstice + 30 d. Note the absence of gray-like tone indicative of surface melt as shown in (a) for the Arctic areas.*

(Cox and Weeks, 1973). Salinity profiles of the Weddell summer pack ice (Ackley and others, 1978) indicate some brine drainage from the upper portion similar to observations on the ice of the Arctic regions, however, unlike the Arctic, the lower-level salinities are still relatively high indicating redistribution of salinity into these lower layers without the nearly complete drainage evident in Arctic summer ice (Meguro and others, 1967; Cox and Weeks, 1973). Table II shows the average salinity of cores taken compared with the average salinity expected for Arctic winter ice and Arctic summer ice obtained by Cox and Weeks (1973). As shown here, (columns 4 and 5) the average salinity of the ice in the Weddell summer pack is nearly that characteristic of Arctic winter ice.

TABLE II. COMPARISON OF AVERAGE SALINITY OF WEDDELL (SUMMER) PACK ICE TO AVERAGE SALINITIES OF ARCTIC WINTER AND SUMMER ICE

| Core samples | Ocean station | Weddell pack ice | | Arctic winter ice ‰ | Arctic summer ice ‰ |
		Thickness m	Average salinity ‰		
22-8	H	4.0	2.75	*	*
22-4	J	3.0	2.83	3.11	2.11
25-9	K	1.2†	5.35	5.97	1.79
27-19	M	1.72†	4.71	5.15	1.88
28-2	N	2.40†	6.28	4.06	2.00
MI-10	O	1.82	3.94	4.99	1.90

* Calculated values are not valid for ice exceeding 3.4 m in thickness.
† Full-length core samples.

All these observations are consistent with a low top-surface ablation inside the summer minimum ice edge. The relatively high accumulation under thick ice in only one year indicated by the south to north thickness difference (Fig. 5) may be accounted for by this lack of summer melt ablation in the western regions. In contrast, while the Arctic case indicates a similar one-year accumulation of 2 m, about 0.4 m is lost there by summer melt (Koerner, 1973) so the next year's accumulation has to make up this summer loss before additional thickness can be added on. The indications are that melt loss from Weddell ice inside the summer edge is quite low as the second winter's accumulation is added directly onto the previous winter's giving a greater net thickness than similarly aged Arctic ice after two years accumulation.

Snow cover

The snow cover can provide significant attenuation of the energy exchange, and, as Maykut (1978) has pointed out, it is especially important over young ice. As shown in Figure 5, little to no snow cover exists on the young ice (<1 m) in the edge region. On the older ice, snow depths were measured and are reported in Figure 10. In general, the snow depths are quite low. Snow densities were not measured directly, but based on resistance during depth measurements were estimated at generally within the 0.2 to 0.3 Mg/m^3 range and not exceeding about 0.35 Mg/m^3. Snow covers of these depths and densities are significant in reducing the energy fluxes over the ice (Maykut, 1978) but depths are less than the values obtained off East Antarctica or in the near-shore fast-ice regions. Off East Antarctica, the snow cover can exceed about one-quarter the ice thickness (>0.5 m) leading to depression of the top surface of the ice below sea-level and surface flooding (Meguro, 1962). High-salinity ice then forms by the infiltration of sea-water into the snow adjacent to the top ice surface.
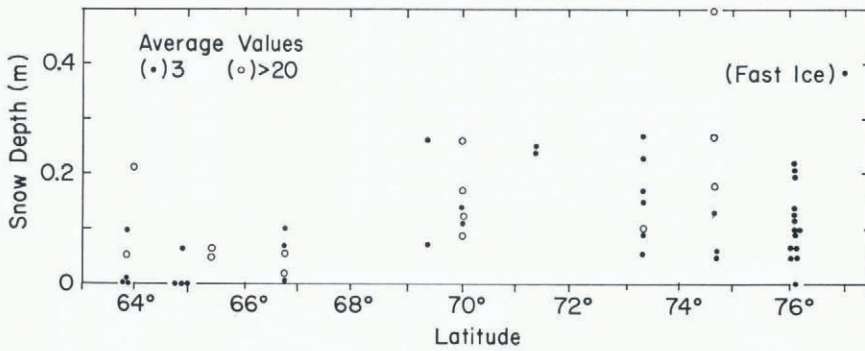
Fig. 10. Snow depth measurements on the Weddell Sea pack ice.

Ice of this structure was not observed in the Weddell field study nor were snow thicknesses >0.5 m seen except on fast ice near the continent and one sample of drifting pack that may have originated as fast ice.

Ice transport

Data on drift rates are limited and from two sources, ship tracks (Brennecke, 1921) of the *Endurance* and *Deutschland* (Fig. 7) and recently tracked icebergs using satellite data (Swithinbank and others, 1977). An example of an iceberg track obtained from ESMR satellite data during 1974–75 is also shown in Figure 7. As shown, the track generally parallels that of the *Deutschland* (up to *c*. 65° S.) some 60 years earlier. Drift rates from the ship and iceberg tracks are shown in Table III.

TABLE III. DRIFT RATES IN THE WEDDELL SEA

	Mean drift rate km/d (m/s)
Endurance	4.1 (0.047)
Deutschland	4.3 (0.050)
Coats Land Iceberg	2.74 (0.032)

Differences in the mean drift may be because the deeper draft of the iceberg allows it to be more affected by deep currents than the surface ships. Daily drift rates exceed these mean rates and can be up to the order of 40 km/day (0.47 m/s) (*Deutschland* drift, 3–6 August 1912). The mean winter drift rate of the *Deutschland* (1 June–31 August 1912) was 7.3 km/d (0.084 m/s), higher than the mean rate over the entire drift, perhaps reflecting stronger winds during the winter period.

A "box" model for the Weddell Sea region

Figure 11 shows a possible breakdown of the larger Weddell Sea region into eight sub-areas based on distinct changes in the ice characteristics between these regions. The ice edge at various times during advance is also indicated. After Barber and others (1977), a "box" model for the ice balance can be constructed and described by the following equations where C_i denotes accumulation for region i, A_i the ablation and $G_{i,j}$ the transport across the boundary between region i and region j so that B_i is then the balance of ice in i, all quantities taken over time interval Δt. The simplified set of equations are:

$$
\left.
\begin{array}{ll}
C_1 - G_{1,\,2} = B_1 & \text{(a)} \\
C_2 - A_2 + G_{1,\,2} - G_{2,\,3} = B_2 & \text{(b)} \\
C_3 - A_3 + G_{2,\,3} - G_{3,\,6} = B_3 & \text{(c)} \\
C_4 - A_4 - G_{4,\,5} + G_{4,\,7} = B_4 & \text{(d)} \\
C_5 - A_5 + G_{4,\,5} - G_{5,\,6} + G_{5,\,7} = B_5 & \text{(e)} \\
C_6 - A_6 + G_{5,\,6} + G_{3,\,6} - G_{6,\,8} = B_6 & \text{(f)} \\
C_7 - A_7 - G_{7,\,8} - G_{5,\,7} - G_{4,\,7} = B_7 & \text{(g)} \\
C_8 - A_8 + G_{7,\,8} + G_{6,\,8} = B_8 & \text{(h)}
\end{array}
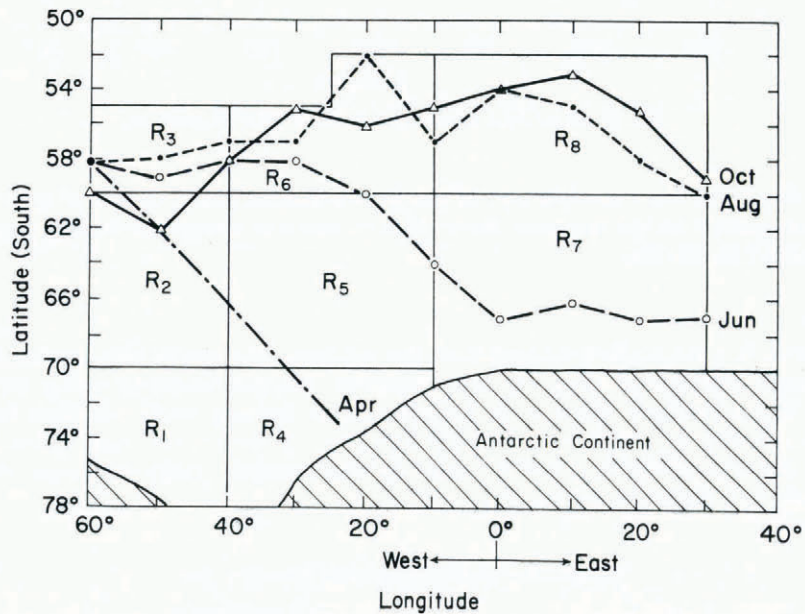\right\}, \qquad (1)
$$

Fig. 11. Divisions of the Weddell Sea region into eight sub-areas for mass-balance purposes (Equations (1)).

The equations reflect the trend of transport shown for the drift track of the ships (Fig. 7) and in the ocean currents (Gordon and others, 1978). The magnitudes of the $G_{i,\,j}$'s (transport) would be greatest for the regions north of lat. 60° S. where the winds in the southern hemisphere markedly increase (Regions R_5, R_6, and R_8). It is also expected that accumulation will be highest in the southern and less in the northern regions. However, deformation depends on wind strengths and fluctuations and can be highly significant in altering this accumulation relation. Ablation terms, on the other hand, could probably be calculated knowing the general seasonal trends of the energy balance at the surface, but a significant term is probably the ice melting from the sides during lesser concentration in summer, again a function of the unknown deformation history.

The present calculation of the balance, therefore, is hampered by the lack of complete transport information (only $G_{1,\,2}$ and $G_{2,\,3}$ are known from historical ship drifts) and the unknown deformational component of the accumulation and ablation terms in each region. The complete regional balance calculation, therefore, can only be done accurately when detailed wind-driving information and verification by ice-strain and drift networks are both available. It is hoped that an array of drifting buoys emplaced in 1979 will provide this information.

MASS BALANCE AND ASSOCIATED SALT FLUX OVER THE CONTINENTAL SHELF

Gill (1973) offers an explanation for the presence of high-salinity water on the continental shelf associated with freezing and transport of sea ice over this region (R_I in Fig. 11). The relatively simple mass balance (Equation (1a)) for this region allows a check on the quantities derived. In Gill's simple model, a Stefan growth law for ice based on observed rates of freezing near the ice shelf (Foster, 1972) is given as

$$\eta = 4 \times 10^{-4} t^{\frac{1}{2}}, \tag{2}$$

with η in meters and t in seconds.

Since ice moves away from the shore with a speed U, as shown on the ship drift tracks (Fig. 7); ice at distance x where $x < Ut$ will have thickness

$$\eta = 4 \times 10^{-4} (x/U)^{\frac{1}{2}}, \qquad x < Ut, \tag{3}$$

while

$$\eta = 4 \times 10^{-4} t^{\frac{1}{2}}, \qquad x > Ut.$$

The rate of brine release depends on the local growth-rate

$$\left. \begin{array}{ll} \dot{\eta} = 2 \times 10^{-4} t^{-\frac{1}{2}}, & t < x/U \\[2mm] \dot{\eta} = 2 \times 10^{-4} (x/U)^{-\frac{1}{2}}, & t > x/U. \end{array} \right\} \tag{4}$$

The *average* rate of brine release over $L < Ut$ is equivalent to freezing a thickness

$$\bar{\eta} = \tfrac{4}{3} \times 10^{-4} (L/U)^{\frac{1}{2}} + 4 \times 10^{-4} (U/L)^{\frac{1}{2}} t. \tag{5}$$

From the *Endurance* drift, $U/L = 6$ months where L is the distance to the edge of the continental shelf. Based on these estimates, Gill then obtains a brine release equivalent to the production of an average ice thickness of about 2.1 m during the winter season less an assumed 0.4 m loss during summer melt, or an annual production of 1.7 m.

We may update this quantity by considering that there is little to no ablation (as indicated in the balance formulation (Equation (1a)) to lower the average ice thickness. The 2.1 m would therefore remain intact without melt losses. Similarly, the indications are for sub-freezing air temperatures well into the summer period, so continuing, but lowered, growth during the summer half-year is probably in order and indicated by thin ice of *c*. 1 m thickness observed during the field study at the end of the summer. The total annual production is therefore estimated at an average of approximately 3.1 m, 2.1 m for the winter six months and 1 m for the summer. Additionally, deformation would also enhance the production by ridging the thinner ice and exposing additional open water. From Figure 8, ridged ice accounts for *c*. 17% of the total and is of thickness >4 m and therefore would roughly add (0.17 × 4 m) or *c*. 0.6 m to the average thickness. The average thickness formed on an annual basis over the shelf could therefore be of the order of 3.7 m or roughly twice the amount assumed earlier.

In this earlier study, some estimates were made of the amounts of salt flux created by the ice that were removed by the horizontal and vertical water circulations. If the higher estimate of ice thickness given here is used, these fluxes would be commensurately higher necessitating, after Gill (1973), a faster horizontal exchange of shelf water of the order of 1.5 years compared to about 3.5 years. This contribution would considerably increase our estimates of Bottom Water production in the Weddell Sea. The high end of the range of the Weddell Sea Bottom Water flow estimated by Foster and Carmack (1976) (5×10^6 m³/s) from oceanographic data may, therefore, be more applicable than the lower rate (2×10^6 m³/s) based on the assumed lower sea-ice production rates given previously.

REFERENCES

Ackley, S. F. 1977. Sea ice studies in the Weddell Sea region aboard USCGC *Burton Island*. *Antarctic Journal of the United States*, Vol. 12, No. 4, p. 172–73.
Ackley, S. F., *and* Keliher, T. E. 1976. Antarctic sea ice dynamics and its possible climatic effects. *AIDJEX Bulletin*, No. 33, p. 53–76.
Ackley, S. F., *and others*. 1978. Primary productivity in sea ice of the Weddell region, by S. F. Ackley, S. Taguchi, and K. R. Buck. *U.S. Cold Regions Research and Engineering Laboratory. Report* 78-19.
Barber, F. G., *and others*. 1977. Beaufort Sea box model of ice, by F. G. Barber, J. Duck, W. E. Markham, and T. S. Murty. *Canada. Dept. of Fisheries and the Environment. Marine Sciences Directorate. Manuscript Report Series*, No. 43, p. 255–58.
Brennecke, W. 1921. Die ozeanographischen Arbeiten der Deutschen Antarktischen Expedition 1911–1912. *Archiv der Deutschen Seewarte*, 39. Jahrg., Nr. 1.
Bunt, J. S. 1963. Diatoms of Antarctic sea ice as agents of primary production. *Nature*, Vol. 199, No. 4900, p. 1255–57.
Cox, G. F. N., *and* Weeks, W. F. 1973. Salinity variations in sea ice. *U.S. Cold Regions Research and Engineering Laboratory. Research Report* 310.
Deacon, G. E. R. 1977. The cyclonic circulation in the Weddell Sea. *Deep Sea Research*, Vol. 23, No. 1, p. 125–26.
Foster, T. D. 1972. Haline convection in polynyas and leads. *Journal of Physical Oceanography*, Vol. 2, No. 4, p. 462–69.
Foster, T. D., *and* Carmack, E. C. 1976. Frontal zone mixing and Antarctic bottom water formation in the southern Weddell Sea. *Deep Sea Research*, Vol. 23, No. 4, p. 301–77.
Gill, A. E. 1973. Circulation and bottom water production in the Weddell Sea. *Deep Sea Research*, Vol. 20, No. 2, p. 111–40.
Gordon, A. L., *and others*. 1978. Large scale relative dynamic topography of the Southern Ocean, [by] A. L. Gordon, E. Molinelli, and T. Baker. *Journal of Geophysical Research*, Vol. 83, No. C6, p. 3023–32.
Hibler, W. D., III. 1979. A dynamic-thermodynamic sea ice model. *Journal of Physical Oceanography*, Vol. 9, No. 4, p. 815–46.
Koerner, R. M. 1973. The mass balance of the sea ice of the Arctic Ocean. *Journal of Glaciology*, Vol. 12, No. 65, p. 173–85.
Maykut, G. A. 1978. Energy exchange over young sea ice in the central Arctic. *Journal of Geophysical Research*, Vol. 83, No. C7, p. 3646–58.
Meguro, H. 1962. Plankton ice in the Antarctic Ocean. *Nankyoku Shiryō: Antarctic Record*, [No.] 14, p. 72–79.
Meguro, H., *and others*. 1967. Ice flora (bottom type): a mechanism of primary production in polar seas and the growth of diatoms in sea ice, by H. Meguro, K. Ito, and H. Fukushima. *Arctic*, Vol. 20, No. 2, p. 114–33.
Swithinbank, C. W. M., *and others*. 1977. Drift tracks of Antarctic icebergs, by C. [W. M.] Swithinbank, [E.] P. McClain, and P. [M.] Little. *Polar Record*, Vol. 18, No. 116, p. 495–501.
Thorndike, A. S., *and others*. 1975. The thickness distribution of sea ice, [by] A. S. Thorndike, D. A. Rothrock, G. A. Maykut, and R. Colony. *Journal of Geophysical Research*, Vol. 80, No. 33, p. 4501–13.
Zwally, H. J., *and* Gloersen, P. 1977. Passive microwave images of the polar regions and research applications. *Polar Record*, Vol. 18, No. 116, p. 431–50.

DISCUSSION

G. DE Q. ROBIN: May not the difference from Arctic pack ice be due to melting of ice floes from below by sensible heat from sea-water? Floes in northerly belts of Antarctic pack ice are much more broken by wave action than in the Arctic. When these spread out you have a large proportion of open water to absorb solar heat (often 20 to 80% open water) but floes maintain a high albedo due to snow cover. This may well make melting from below the dominant process in contrast to Arctic ice.

S. F. ACKLEY: I would agree completely with this mechanism, and we observed this melting mechanism frequently during the field study. However, this type of ablation does not apply inside the summer minimum ice edge since the wave damping by the ice edge is so severe. If, as Dr Robin and I apparently agree, the primary ablation in the Weddell pack is by the sensible heating from solar-warmed sea-water, then the conclusion is that ablation inside the summer minimum ice edge must be low because the high concentration of sea ice prevents both the heating of the water in openings and the wave action necessary to complete the melting. That is the conclusion reached independently by the physical properties of ice shown in Figures 13 and 14 and by the salinity data in Table III.

O. ORHEIM: Your suggestion that there is little ablation within the pack ice does not completely agree with our field evidence for the mid-summer period. We saw no freezing except in small amounts near the Filchner Ice Shelf, and although it is true that there is little evidence of melt ponds, etc., many floes are observed to have been thinned and melted, presumably by sea action.

ACKLEY: As discussed also in the comment to Dr Robin, there is no disagreement here, again the conclusion is that in those areas where the ice concentration remains high through the summer period, sea action cannot occur. The conclusion from this study is that for pack ice that survives through the summer period, top-melt ablation is relatively insignificant. In contrast, the typical piece of Arctic ice loses c. 0.4 m (25%) of its thickness by melting during the summer. The conclusion is important because the ice thickness of the older floes in the northern Weddell is relatively thicker than Arctic ice of similar age because it has survived at least one summer season with little ablation.

R. M. KOERNER: You might try comparing the ablation-rates on glaciers on the Antarctic Peninsula and in the Arctic to gain some information of relative Arctic Ocean/Weddell sea-ice ablation rates.

ACKLEY: Thank you for the suggestion; we will attempt this in the near future.